Highly Ordered Nanostructured Magnetite and Maghemite of Micrometric Sized and Rhombohedral Habit

Mihaela Luminita Kiss[1,2], Marius Chirita[1†], Aurel Ercuta[3], Cecilia Savii[4], Adrian Ieta[5]

[1]Department of Nanocrystal Synthesis, NIRDECM, Timisoara, Romania; [2]"Politehnica" University, Timisoara, Romania, [3]Faculty of Physics, West University of Timisoara, [4]Institute of Chemistry Timisoara of Romanian Academy; [5]Department of Physics, SUNY Oswego, NY, USA.†corresponding author: Tel/Fax: +40-256-494413, e-mail: chirifiz@gmail.com

ABSTRACT

We present the case of porous magnetite and vacancy-ordered maghemite crystals of rhombohedron shape and size reaching 150μm synthesized via topotactical conversion, starting from siderite single crystals. The increase in density (from 3.9 g/cm^3 for siderite to 5.24 g/cm^3 for magnetite and to 4.9 g/cm^3 for maghemite) caused quasi-ordered internal pore-grain patterns, with grain arrangement suggesting a mesocrystalline appearance. The microstructure analysis based on X-ray Line-Profile Fitting gave an average inner grain-size of 64 ± 6 nm for magnetite and 84 ± 8 nm for maghemite, in good agreement with the SEM observations. While the crystals exhibit smooth facets, the internal porosity leading to remarkably large specific surface area (88.55 m^2/g for magnetite, and 40.14 m^2/g for maghemite, as evaluated by means of the BET method) suggests a mesocrystalline structure. The sharp peaks in the XRD spectrum (not presented here) indicate high crystallinity. Both iron oxyde crystals exhibit magnetic hysteresis, with saturation magnetization of 92.1 emu/g for magnetite and 85.5 emu/g for maghemite.

Keywords: crystal structure, nanostructures, topotaxy, oxides, magnetic material

1. INTRODUCTION

Synthetic magnetite (Fe_3O_4) and maghemite (γ-Fe_2O_3) of good quality are of increasing interest, due to the large palette of applications of these materials (especially as powders, colloids, gels, composites, thin films or sintered ferrites) in many fields, from chemistry, electronics, and magnetic data storage to earth and life sciences [1-5]. Compared to the case of nanosized crystals, there is only scarce data reported in the literature on the production of micrometric (or larger) crystals of well-defined habit. Although some reports on the obtaining magnetite or maghemite by thermal treatment of siderite exist, none refers to the porosity developed in these oxides subsequent to the conversion. Moreover, there are no reports on highly crystalline iron oxides of internal porosity, but maintaining the habit of the single crystal polyhedrons of the siderite precursor.

Wang [6] proved that conversion of the siderite to hematite (via magnetite) is topotactical, but he neither did make any statement or observation on the porosity developed in as-obtained iron oxides, nor explained the observed fact that the diffraction spots of the resulting iron oxide are slightly diffuse compared to the educt.

We have recently proposed [7,8] a novel synthesis route of submillimeter-sized siderite single crystals of rombohedron habit, based on the hydrothermal decomposition of the Fe-ethylenediamine-tetraacetic acid complex (Fe(III)-EDTA); the present contribution provides complementary informations to a recently published article [9] reporting on the successive conversion of the thus-synthesized siderite to pure magnetite and vacancy-ordered maghemite, by heating under specific conditions.

2. EXPERIMENTAL METHODS

2.1. Synthesis

Chemicals: $FeNH_4(SO_4)_2 \cdot 12H_2O$ (FAS), Na_4EDTA and $(NH_2)_2CO$ (urea), of analytical purity were supplied by Fluka (Sigma-Aldrich). Synthesis of the iron carbonate ($FeCO_3$) was carried out according to the following procedure: we prepared an aqueous solution**:** 1.05×10^{-1}M of FAS, 1.05×10^{-1}M Na_4EDTA and $9.71 \cdot 10^{-1}$M urea. The pH of the final solution was initially set to approx. 6 by HCl addition; the red color of the solution indicated the formation of the Fe(III)EDTA complex. The solution was transferred into a Teflon-lined stainless-steel autoclave, then heated up to 250ºC by a rate of 1.7ºC/min, and maintained for 22h. After this time, the autoclave was rapidly cooled in water. The pH measurement indicated a value between 9.38 and 9.53 of the remaining solution. The resulting $FeCO_3$ microparticles with size in the range of 150μm-200μm were filtrated, washed with bidistilled water and dried at 60°C in air.

Conversion of $FeCO_3$ to Fe_3O_4 was done inside a quartz tube heated for 2h at 450ºC, under Ar flow (1ml/s), while

conversion of Fe_3O_4 to γ-Fe_2O_3 was done by mantaining the as-resulting magnetite for 7h at 270ºC in air.

2.2. Characterization

An X'Pert PRO MPD difractometer (PANalytical) with Cu Kα radiation (λ=0.15418 nm, Ni filter), θ configuration, assisted by the X'Pert Data Collector program was used for the analysis of crystal structure at room temperature. The PDF 4+ Database of Joint Committee on Powder Diffraction Standards (JCPDS) was used for phase identification. SEM and FEI (Inspect S) were employed for the morphology of the particles and energy-dispersive X-ray spectroscopy (EDAX) analysis for the identification of chemical components. Infrared (IR) spectrum was recorded within the $4000cm^{-1}$-$400cm^{-1}$wave number range, by means of a JASCO 4200 Fourier transform infrared (FT-IR) Spectrophotometer using a KBr wafer. An ac hysteresigraph [10] was used to test the magnetic properties of the particles.

3. RESULTS AND DISCUSSION

The morphology of the microcrystals and the crystallite size in the range of 150 - 200 μm was evaluated from the SEM image (Figure 1).

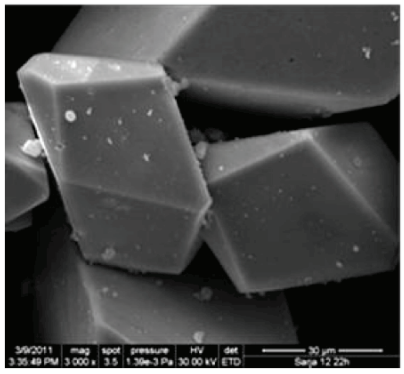

Figure 1. The SEM images of the $FeCO_3$ microcrystals

The X-ray diffraction spectrum (shown in figure 2) allowed unequivocal identification of the iron carbonate crystalline pattern; all the diffraction peaks were indexed to $FeCO_3$, in

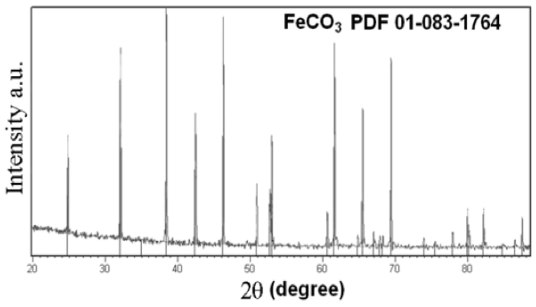

Figure 2. The XRD spectrum of the $FeCO_3$ microcrystals

agreement with the ICSD (Inorganic Crystal Structure Database) reference code: 01-083-1764.

Phase transition

In order to detect the temperature at which the siderite-to-magnetite phase transformation (thermally activated) starts, a sample from the $FeCO_3$ powder was extracted and heated under dynamic vacuum conditions, between 25º C and 500º C (2deg/min heating rate), inside the high temperature chamber attached to the difractometer; the records at 350º C, 400º C and 500º C are shown in Figure 3. These spectra clearly show that the phase transition starts in the proximity of 400º C.

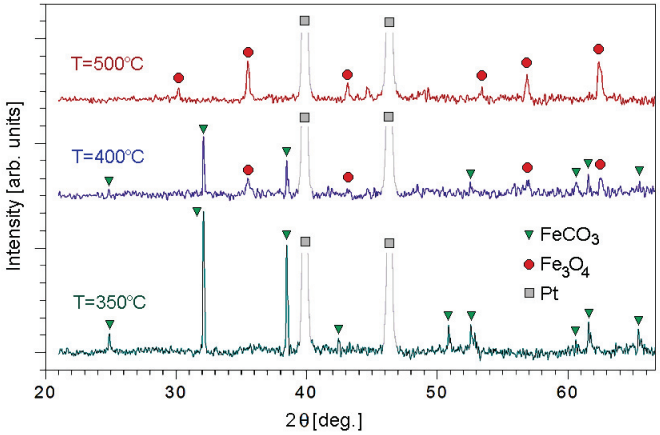

Figure 3. XRD $FeCO_3$-Fe_3O_4 transition kinetics; the gray peaks (truncated) correspond to the platinum sample holder

After conversion of $FeCO_3$ to Fe_3O_4, (Fig. 4a) and the conversion of Fe_3O_4 to γ-Fe_2O_3, the recorded diffraction peaks (not shown) were found to match the cubic Fe_3O_4 space group $Fd\bar{3}m$ (227) pattern (ICSD 01-088-0315, a=b=c=8.3750Å-JCPDS Database) and the tetragonal (vacancy - ordered superlattice) γ-Fe_2O_3 space group P pattern (ICSD 00-025-01402, a=b=8.3400 Å, c=25.0200 Å - JCPDS Database), respectively. The sharpness and strength of the diffraction peaks are also indicative for high crystallinity [11].

The SEM (Fig. 4b), confirm that both the Fe_3O_4 and γ-Fe_2O_3 crystals practically exhibit the same rhombohedral habit, size and smooth facets; from a comparison with the $FeCO_3$ educt crystals it resulted that, as expected, no morphological change occurred during topotactical conversion. In addition, the increase in density (from 3.9 g/cm^3 for siderite to 5.24 g/cm^3 for magnetite and 4.9 g/cm^3 for maghemite) led to a porous structure, as Figure 4c confirms for magnetite and Figure 4d confirms for maghemite. Inside the broken crystals, 70 nm - 80 nm magnetite grains forming a quasi-ordered pattern are clearly visible; together with the fact that the oxide crystals resulted from topotactical solid state reactions; this suggests a mesocrystalline arrangement [12, 13]. The maghemite grains were found to be somewhat larger than those of magnetite (50 nm - 60 nm), presumably due to new cells formation. According to [12], mesocrystals

are highly crystalline structures, defined as crystals that are built up from individual nanocrystals aligned in a common crystallographic register. These mesocrystals can be obtained by different laborious methods, usually based on orientated aggregation of nanocrystals, followed by thermal treatment, but they can be obtained easily via topotactic

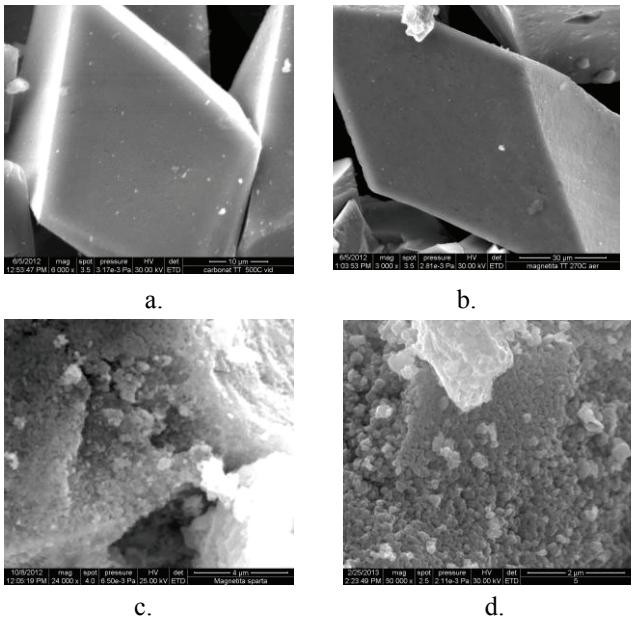

Figure 4. SEM images of the Fe_3O_4 (a) and γ-Fe_2O_3 (b) crystals, and details from the inside of a crushed crystal of Fe_3O_4, (c) and γ-Fe_2O_3 (d) revealing porosity and granulation.

solid state reaction, when the expected density of the final product is higher than that of the educt. Mesocrystals usually scatter X-rays like a single crystals, thus being

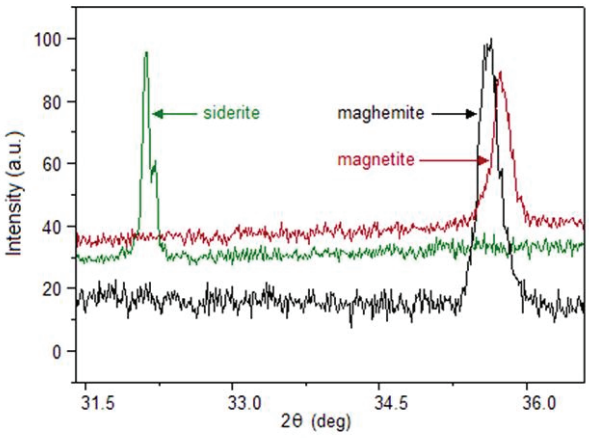

Figure 5. Comparison between siderite and magnetite/ maghemite XRD patterns

difficult to distinguish from these; however, a slight broadening of the diffraction peaks can indicate the transformation of the single crystalline structure into a mesocrystalline structure.

Microstructure analisys of the XRD patterns was performed by Line-Profile analysis using the XFit software. In our case, from the structure viewpoint [6], the unit cell of the cubic Fe_3O_4 had the same orientation relationship with the $FeCO_3$ rhombohedral parent phase, i.e. $[111]_m//[001]_s$, and $[2\text{-}1\text{-}1]_m//[120]_s$. ("m" and "s" denote magnetite and siderite, respectively). This topotactic transformation accompanied by the increase of crystals' theoretical density from 3.9g/cm^3 for siderite to 5.3g/cm^3 for magnetite (extracted from the crystallographic parameters of the indicated patterns) suggest that crystallites must be appear. On the other hand, the visual comparison (Fig. 5) between siderite and magnetite/ maghemite XRD patterns shows that peks of the magnetite/ maghemite are broader than siderite.

The standard pattern was used together with samples pattern using the same refining codes for instrumental parameters. The average crystallite size was calculated using the same refining code for all the peaks in the pattern. The procedure was also used for the stress contribution. The results (the average dimensions of crystallites and the strain) are presented in table 1.

Sample	Size (nm)	Strain (%)
Magnetita	64 ± 6	0.237 ± 0.025
Maghemite	84 ± 8	0.000

Table 1. Average dimensions of crystallites and the strain for magnetite and maghemite

This qualitative analysis regarding internal structure indicates that our crystals are built up from individual nanocrystals aligned in a common crystallographic register corresponding to mesocrystalline structure.

The FT-IR analysis (Fig. 6) was carried out in order to identify the magnetite by checking the presence of both the Fe–O bond and of the magnetite skeleton vibrations. Thus, a characteristic absorption band of the Fe–O in Fe_3O_4 was detected at 570.82cm^{-1}. In addition, the absorption peaks

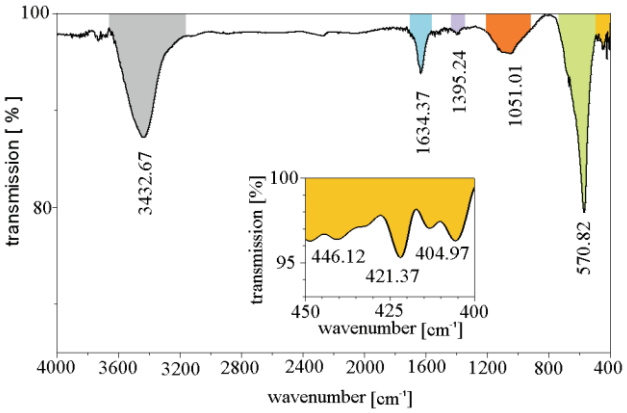

Figure 6. The FT-IR spectrum of magnetite (the blue band)

detected in the vicinity of 405 cm^{-1} are also characteristic to magnetite. The band at 446.12 cm^{-1} is characteristic to the Fe–O vibrations. The IR band at 1051 cm^{-1} it can indicate that sample contains a specifically adsorbed sulphate groups (from the initial precursor), which occupy external surfaces in magnetite microparticles. The 1395.24 cm^{-1} IR feature could be due to both $\nu_s(COO^-)$ free (1405 cm^{-1}) and $\nu_s(COO^-)$, as Nowak and coworkers observed [14]. According to Lu [15], the peak at 1634,37 cm^{-1} corresponds to Fe–O (1624 cm^{-1}). A wide and strong absorption band (3100–3630 cm^{-1}) centered at 3432.67cm^{-1} was assigned to O–H vibrations.

The two oxide products exhibit a normal ferromagnetic-like behavior (hysteresis) at room temperature, with moderate values of the coercivity and remanence. The magnetic behaviour of magnetite (Fig. 7) indicate a saturation magnetization of 95.5 emu/g, aproaching the maximum values reported for the bulk in the litterature. The saturation

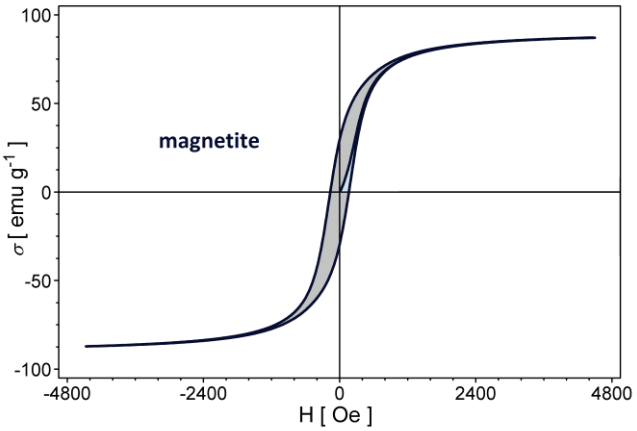

Figure 7. The normal magnetization curve and the hysteresis loop of the magnetite crystals

magnetization of the maghemite crystals was found to be 87.3emu/g (the hysteresis loop not shown here), by approx. 9% lower compared to the magnetite. Both these values are indicative for high purity.

4. CONCLUSIONS

After the thermal treatment of micrometric $FeCO_3$ single crystals, the obtained magnetite and maghemite exhibiting smooth facets, have internal porosity leading to remarkably large specific surface area (88.55 m^2/g for magnetite, and as 40.14 m^2/g for maghemite as evaluated by means of the BET method-figures not presented here). Both Fe oxyde crystals exhibit magnetic hysteresis with saturation magnetization (92.1 emu/g for magnetite and 85.5 emu/g for maghemite). The increase in density, the topotactic transformation and the internal grain arrangement (from SEM), suggests a mesocrystalline internal structure for magnetite and maghemite. The present results have demonstrated the possibility of obtaining porous rhombohedral submillimeter-sized magnetite and maghemite crystals having remarkably large specific surface area, usually associated with crystallites with nanometric dimensions; this property associated with their large dimensions (150μm) and with their highly crystallinity (as if it were a single crystal) could be extremely useful in a large aria of application, especially where magnetic carriers with enough specific surface area of reactivity are needed.

AKNOWLEDGEMENTS

This work was supported by the program PN 09 34 01 01 of the Romanian Ministry of Research and Education. Helpful discussions and technical support from Dr R. Banica, Dr P. Sfirloaga and R. Baies (all from NIRDECM) are kindly aknowledged.

REFERENCES

[1] Coey, J.M.D. *Magnetism and Magnetic Materials*. Cambridge Univ. Press, New York, 2009; Chapter 1, pp 13-15.

[2] E du Tremolet de Lacheisserie, E.; Gignoux, D.; Schlenker, M.; *Magnetism Materials & Applications*. Springer Science Business Media Inc., Boston, 2005; Vol. 2.

[3] Majewski, P.; Thierry, B. *Crit. Rev. Solid State*. **2007**, *32*, 203-215.

[4] Bao, N.; Gupta, A. J. Mater. Res. 2011, 26, 2, 111-121.

[5] Cornell, R. M.; Schwertmann, U. The Iron Oxides: Structure, Properties, Reactions, Occurences and Uses. **2003**, Wiley-VCH Verlag GmBT & Co, KgaA, Winheim ISBN: 3-527-30274-3.

[6] Wang, J.; Sakakura, T.; Ishizawa, N.; Eba, H. J. Symposium 1: Advanced Structural Analysisand Characterization of Ceramics Materials IOP Publishing IOP Conf. Series: *Mater. Sci. Eng*. **2011**, 18, 022011 doi: 10.1088/1757-899X/18/2/022011.

[7] Chirita, M.; Ieta, A. *Cryst. Growth Des*. **2012**, *12*, 883−886.

[8] Chirita, M.; Banica, R.; Ieta, A.; Bucur, A.; Sfirloaga, P.; Ursu, D. H.; Grozescu, I. *AIP Conf. Proc*. **2010**, *1262*,124.

[9] A. Ercuta, M. Chirita, Highly Crystalline Porous Magnetite and Vacancy Ordered Maghemite of Rhombohedral Habit; J. Cryst Growth, 2013, Vol. 380, pp.182-186.

[10] I. Mihalca and A. Ercuta, *J Optoelectron Adv M* 5, (2003), p. 245.

[11] Qi, H.; Ye, J.; Tao, N.; Wen, M.; Chen, Q. *J. Cryst. Growth*. ***2009***, *311*, 394-398.

[12] Cölfen, H.; Antonietti, M. *Mesocrystals and non-classical crystallization*. John Wiley & Sons Ltd: Chichester, UK 2008, pp 159-163.

[13] Rui-Qi, S.; Cölfen, H. Adv. Mat. **2010**, 22, *12*, 1301-1330.

[14] B. Nowack, J. Lutzenkirchen, P. Behra, and L. Sigg. *Environ Sci Technol* 30 (1996), p. 2397–2405.

[15] W. Lu, Y. Shen, A. Xie, and W. Zhang, *J Magnetism and Magnetic Materials* 32, (2010), p. 1828-1833.